Solid state and solution structures of two structurally related dicopper complexes with markedly different redox properties

Peter Comba,*,†,[a] Trevor W. Hambley,[b] Peter Hilfenhaus[a] and David T. Richens*,[c]

[a] *Anorganisch-Chemisches Institut, Universität Heidelberg, Im Neuenheimer Feld 270, 69120 Heidelberg, Germany*

[b] *School of Chemistry, University of Sydney, Sydney, NSW 2006, Australia*

[c] *School of Chemistry, University of St. Andrews, The Purdie Building, St. Andrews KY16 9ST, UK*

The dinuclear dicopper(I) complex of a 26-membered macrocycle, L^1, obtained from the 2 + 2 condensation of terephthalaldehyde and 3-azapentane-1,5-diamine, has been isolated as an air stable red-orange complex in good yield. The crystal structure of $[Cu_2(NCMe)_2L^1][ClO_4]_2$ [triclinic, space group $P\bar{1}$, a = 10.5773(9), b = 10.8385(8), c = 7.9715(4) Å, α = 99.572(6), β = 91.698(7), γ = 108.952(6)°] showed two distorted tetrahedrally co-ordinated copper(I) centres with a Cu–Cu separation of 7.04 Å. The air stability of $[Cu_2(NCMe)_2L^1]^{2+}$ contrasts with the oxygen sensitivity of the dicopper(I) complex of the 24-membered macrocycle L^3 (2 + 2 condensation of isophthalaldehyde and 3-azapentane-1,5-diamine) which leads to oxygenation of one of the aromatic rings. The marked difference in reactivity is discussed on the basis of the structural differences between the two isomeric compounds, analysed with molecular mechanics calculations. The dinuclear dicopper(II) complexes of the 24- and 26-membered macrocyclic hexaamines L^2 and L^4, derived by reduction of L^1 and L^3, respectively, exhibit dipole–dipole coupling in their EPR spectra. The solution structures of the two dicopper(II) complexes have been determined by a combination of molecular mechanics calculations and the simulation of their EPR spectra.

Haemocyanin, the oxygen carrying protein of the phylla arthropoda and mollusca, and tyrosinase, a related enzyme system that *ortho* hydroxylates phenols (tyrosine) to catechol and ultimately to an *ortho*-quinone, are now established as containing two strongly interacting (type III) copper atoms.[1] Tyrosinase has two copper(I) centres each bound to three histidine nitrogens and separated by 3.6 Å.[1] In an effort better to understand the structure and reactivity of these metalloproteins, many studies have been directed toward synthesizing small-molecule model compounds[1–6] with similar chromophores and to study their spectroscopy and reactivity. Dicopper complexes which bind dioxygen reversibly[7,8] have been studied as models for haemocyanin, and a number of dinuclear copper model complexes catalyse the oxidation of organic substrates.[9,10] Dinuclear copper(I) complexes of macrocyclic ligands with xylyl bridging units which react with dioxygen under hydroxylation of the aromatic ring form a family of successful model compounds for tyrosinase-type reactivity.[11–14]

The macrocyclic ligands L^1 and L^3 are obtained in high yield from a 2 + 2 dipodal condensation of tere- or iso-phthalaldehyde and 3-azapentane-1,5-diamine. Hydrogenation of the imine groups of L^1 and L^3 yields the reduction products L^2 and L^4. Dicopper(I) complexes of L^1 are air stable while those of L^2 cannot be isolated in the presence of oxygen because of the rapid oxygenation of the copper(I) centres and subsequent hydroxylation of one of the benzene rings.[14] The crystal structure of $[Cu_2(NCMe)_2L^1][ClO_4]_2$ is reported and compared with the calculated structure (molecular mechanics) of $[Cu_2L^3]^{2+}$. In contrast to L^1 and L^3 the hexaamines L^2 and L^4 form stable dinuclear Cu^{II} complexes. The solution structures of these weakly coupled dicopper(II) complexes were determined with a combination of molecular mechanics calculations in conjunction with the simulation of the EPR spectra, involving as parameters the Cu–Cu separation and the relative orientation of the two Cu chromophores.[15] The spectroscopic and electrochemical properties and the reactivities of the four dinuclear compounds are discussed on the basis of the structural properties of these compounds.

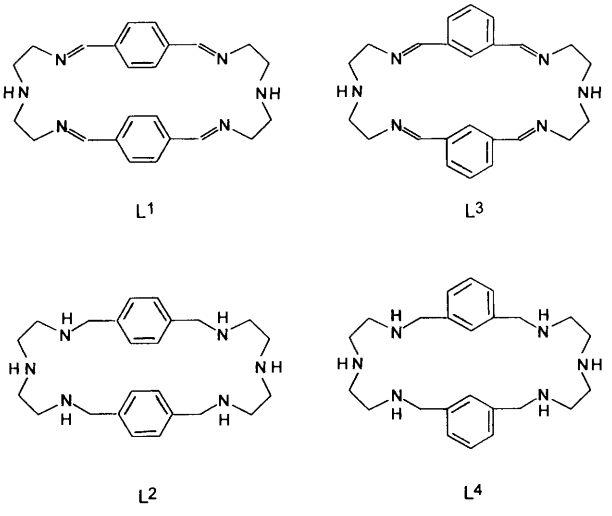

Results and Discussion

Crystal structure of $[Cu_2(NCMe)_2L^1][ClO_4]_2$

The crystallographic analysis confirms the co-ordination of the hexadentate 26-membered macrocycle to two copper(I) ions. In addition, an acetonitrile molecule is co-ordinated to each of the copper(I) centres, completing a severely distorted tetrahedral geometry. The two perchlorate anions do not interact with the metal centres. The separation between the two copper(I) atoms is 7.04 Å. The two benzene rings of the macrocyclic ligand are

† Fax: +49 (6221) 563617. E-Mail: comba@akcomba.oci.uni-heidelberg.de

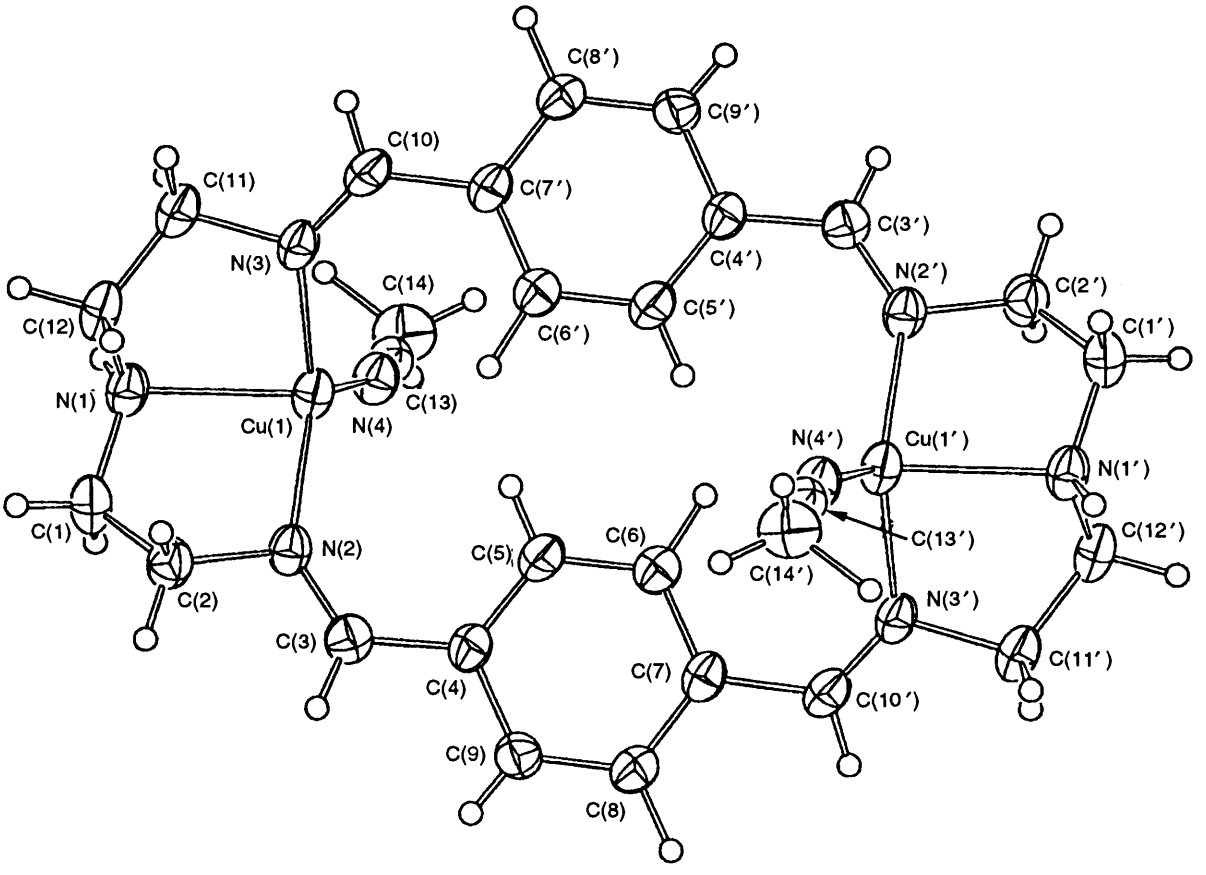

Fig. 1 ORTEP[16] plot of the experimentally determined structure of $[Cu_2(NCMe)_2L^1][ClO_4]_2$

nearly coplanar and in the plane of the four imine donor atoms. The molecular cation of $[Cu_2(NCMe)_2L^1][ClO_4]_2$ is shown in Fig. 1. Positional parameters and selected bond distances and valence angles are given in Tables 1 and 2.

Strain-energy minimized structures of $[Cu_2L^3]^{2+}$ and $[Cu_2L^1]^{2+}$

The two isomers $[Cu_2L^1]^{2+}$ and $[Cu_2L^3]^{2+}$ have markedly different reactivities towards dioxygen. While the structurally characterized $[Cu_2L^1]^{2+}$ is oxygen stable $[Cu_2L^3]^{2+}$ mimics tyrosinase. Its reaction with dioxygen leads to hydroxylation of one of the *meta*-phenylene links. Because of the marked oxygen sensitivity of $[Cu_2L^3]^{2+}$, it has thus far proved impossible to obtain a stable crystalline sample for structural analysis. Therefore, we have analysed the two structures, $[Cu_2L^1]^{2+}$ and $[Cu_2L^3]^{2+}$, with molecular mechanics, using a published force field,[17] with additional parameters fitted to $[Cu_2(NCMe)_2L^1]^{2+}$ and the few relevant copper(I) structures available in the literature. [A search of the Cambridge Structural Data Base revealed that only three structures with a similar chromophore are available; the four structures used for the force-field parameterization include dinuclear copper(I) species with markedly different copper–copper distances, as well as a mononuclear compound, and cover a large enough range of metal–ligand bond lengths for a reasonable force-field parameterization, see Tables 3 and 4.[18–20]]

For simplicity, MeCN has been replaced by NH_3 in $[Cu_2(NCMe)_2L^1]^{2+}$. This reduced the number of force-field parameters to be evaluated and, more importantly, convergence problems are avoided which may be caused by the tumbling of the tail of the co-ordinated acetonitrile. However, calculations with Cu–NCMe geometries constrained to the experimentally observed values indicated that the calculated structure is largely independent of the exact nature of the monodentate ligand. Table 4 shows that the Cu^I–L and Cu^I–Cu^I distances are well reproduced, with the exception of the Cu^I–N_{imine} bond lengths of $[Cu_2L^6]^{2+}$. However, in this structure the copper–imine distances vary over a wide range (2.054–2.120 Å) and the experimental error limits are relatively high (R = 0.084). Also, in general, the angular geometries are well reproduced ($\approx \pm 3°$ for N_{imine}–Cu^I–N_{imine}), except for angles of chromophores with co-ordinated solvent molecules, where distortions of up to 15°

Table 1 Positional parameters for $[Cu_2(NCMe)_2L^1][ClO_4]_2$

Atom	x	y	z
Cu(1)	0.213 34(7)	0.766 35(7)	0.333 65(9)
Cl(1)	0.266 8(1)	0.217 8(1)	0.239 2(2)
O(1)	0.303 7(4)	0.356 0(4)	0.259 5(6)
O(2)	0.137 9(5)	0.150 6(5)	0.163 4(8)
O(3)	0.286 6(6)	0.175 2(6)	0.386 3(7)
O(4)	0.351 1(6)	0.178 7(6)	0.127 7(9)
N(1)	0.364 7(4)	0.891 2(4)	0.196 6(5)
N(2)	0.358 7(4)	0.692 0(4)	0.389 0(5)
N(3)	0.092 5(4)	0.725 8(4)	0.112 4(5)
N(4)	0.161 0(4)	0.876 1(4)	0.520 6(5)
C(1)	0.490 2(6)	0.873 8(6)	0.249 1(8)
C(2)	0.466 7(6)	0.732 5(6)	0.274 8(8)
C(3)	0.384 2(5)	0.633 2(5)	0.504 6(7)
C(4)	0.291 7(5)	0.572 1(4)	0.622 6(6)
C(5)	0.157 6(5)	0.564 5(5)	0.621 5(7)
C(6)	0.071 9(5)	0.492 2(5)	0.724 2(7)
C(7)	0.120 0(5)	0.425 8(4)	0.833 2(6)
C(8)	0.255 3(5)	0.446 3(5)	0.850 7(6)
C(9)	0.340 1(5)	0.516 6(5)	0.744 2(7)
C(10)	−0.029 9(6)	0.660 9(5)	0.066 5(7)
C(11)	0.164 5(6)	0.816 6(6)	0.000 2(7)
C(12)	0.311 9(6)	0.836 9(5)	0.018 5(7)
C(13)	0.141 7(5)	0.958 0(5)	0.606 7(6)
C(14)	0.117(1)	1.070 7(9)	0.715(1)

were observed. This is a general problem for the geometry optimization involving monodentate ligands co-ordinated to metal ions. Especially reassuring is the fact that there is good agreement between the calculated and observed structures of $[Cu_2(Y)_2L^1]^{2+}$ (Y = NH_3 or MeCN, constrained geometries, see above). 120 possible structures of $[Cu_2(Y)_2L^3]^{2+}$ have been refined [s-*cis* or s-*trans* orientation of the imine double bonds; site of co-ordination of the solvent molecule (Y = NH_3); orientation of the secondary amine proton and conformation of the five-membered chelate rings]. From the conformational analysis it emerges that the lowest strain energy structures are a pair of enantiomers (shown in Fig. 2 is the enantiomer with δ conformations of all chelate rings) which are at least 8 kJ mol^{-1} more stable than all the other geometries investigated. The Cu–Cu distance of the minimum energy calculated structure is 3.4 Å, *i.e.* much smaller than that of $[Cu_2(Y)_2L^1]^{2+}$ (6.3 Å, see below), and indeed similar to that of tyrosinase (≈3.6 Å)[1] and that recently found in the crystal structure of oxygenated and deoxygenated haemocyanin (3.6 Å and 4.6 Å).[22] Due to the lack of a reasonable basis for the parameterization we have not attempted to model the peroxo dicopper intermediate formed in the reaction of $[Cu_2(Y)_2L^3]^{2+}$ with dioxygen.[14] A recent crystal structure of haemocyanin from *Limulus polyphemus* points to a μ-η²,η² (side on) binding mode for the bound peroxide.[23] The orientation of the benzene rings {coplanar for $[Cu_2(Y)_2L^1]^{2+}$ and twisted for $[Cu_2(Y)_2L^3]^{2+}$} and the markedly different Cu–Cu separations indicate that the difference in dioxygen reactivity between the two complexes is largely a function of the distance and orientation of the two copper(I) chromophores, and also of the distance of the benzene rings enforced by *meta*- and *para*-substitution in the phenylene backbone.

Table 2 Selected bond lengths (Å) and angles (°) for $[Cu_2(NCMe)_2L^1][ClO_4]_2$

Cu(1)–N(1)	2.185(4)	Cu(1)–N(2)	2.022(5)
Cu(1)–N(3)	2.045(4)	Cu(1)–N(4)	1.957(4)
N(1)–C(1)	1.460(8)	N(1)–C(12)	1.461(7)
N(2)–C(2)	1.482(7)	N(2)–C(3)	1.273(7)
N(3)–C(10)	1.264(6)	N(3)–C(11)	1.482(7)
N(4)–C(13)	1.107(7)	C(1)–C(2)	1.519(9)
C(3)–C(4)	1.456(7)	C(7)–C(10)	1.465(7)
C(11)–C(12)	1.501(9)	C(13)–C(14)	1.47(1)
N(1)–Cu(1)–N(2)	84.6(2)	N(1)–Cu(1)–N(3)	84.4(2)
N(1)–Cu(1)–N(4)	110.4(2)	N(2)–Cu(1)–N(3)	129.2(2)
N(2)–Cu(1)–N(4)	117.7(2)	N(3)–Cu(1)–N(4)	112.7(2)
Cu(1)–N(1)–C(1)	105.0(4)	Cu(1)–N(1)–C(12)	102.2(3)
C(1)–N(1)–C(12)	116.3(5)	Cu(1)–N(2)–C(2)	108.5(4)
Cu(1)–N(2)–C(3)	135.9(4)	C(2)–N(2)–C(3)	115.1(5)
Cu(1)–N(3)–C(10)	134.7(4)	Cu(1)–N(3)–C(11)	107.6(3)
C(10)–N(3)–C(11)	116.4(5)	Cu(1)–N(4)–C(13)	165.3(4)
N(1)–C(1)–C(2)	111.1(4)	N(2)–C(2)–C(1)	110.8(5)
N(2)–C(3)–C(4)	126.4(5)	C(3)–C(4)–C(5)	124.7(5)
C(3)–C(4)–C(9)	117.8(5)	C(6)–C(7)–C(10)	121.3(5)
C(8)–C(7)–C(10)	119.6(5)	N(3)–C(10)–C(7)	124.4(5)
N(3)–C(11)–C(12)	110.2(5)	N(1)–C(12)–C(11)	109.6(5)
N(4)–C(13)–C(14)	177.3(7)		

Table 3 Force-field parameters for mixed amine–imine copper(I) complexes[a]

Bond length parameters

Bond type	Force constant[b]/ mdyn $Å^{-1}$	Strain-free bond length/Å
$Cu(1)–N_{amine}$	0.70	2.000
$Cu(1)–N_{imine}$	0.10	2.200
$N_{imine}=C$	7.20	1.270
$C_{imine}–C_{aromatic}$	5.00	1.460
$C_{imine}–H$	3.90	0.950

Bond angle parameters

Bond angle type	Force constant[b]/ mdyn Å rad^{-2}	Strain-free bond angle/rad
$Cu(1)–N_{imine}–C_{amine}$	0.10	1.912
$Cu(1)–N_{imine}–C_{imine}$	0.10	2.356
$Cu(1)–N_{amine}–C$	0.20	1.920
$Cu(1)–N_{amine}–H$	0.10	1.915
$N_{imine}=C–C_{aromatic}$	0.15	2.094
$N_{imine}–C–C$	0.45	1.911
$N_{imine}=C–H$	0.45	2.094
$N_{imine}–C–H$	0.45	1.911
$C_{imine}–C–C$	0.25	2.094
$C_{imine}=N_{imine}–C$	0.45	2.007
$C_{aromatic}–C_{imine}–H$	0.45	2.094

Torsion angle parameters

Bond torsion	Force constant[b]/ mdyn Å	Offset angle/ rad
$N_{imine}=C^c$	0.0250	1.571
$N_{imine}–C^d$	0.0005	0.524
$C_{imine}–C_{aromatic}{}^c$	0.0100	1.571

[a] Added to the published force field, ref. 16. [b] dyn = 10^{-5} N. [c] Periodicity 2. [d] Periodicity 6.

Solution structures of $[Cu_2L^2]^{4+}$ and $[Cu_2L^4]^{4+}$

The dicopper(II) complexes of L^1 and L^3 are rather unstable (see electrochemical data below). In contrast, the saturated hexaamine ligands L^2 and L^4, produced *via* hydrogenation of the imine groups of L^1 and L^3, form stable complexes with copper(II) in solution. The determination of the solution structures of $[Cu_2L^2]^{4+}$ and $[Cu_2L^4]^{4+}$ is of interest since the EPR spectra of weakly-coupled dicopper(II) complexes may be related to structural parameters and therefore facilitate the molecular mechanics analysis,[15] although the increasing flexibility in the ligand backbone, due to the loss of conjugation, would be expected to lead to different structural properties of the dinuclear compounds. The EPR spectra of $[Cu_2L^2]^{4+}$ and $[Cu_2L^4]^{4+}$ (see Fig. 3) are typical for weakly-coupled dicopper(II) systems.

The structural analysis of the two complexes is based on the MM-EPR procedure used successfully for other dicopper(II) complexes,[15,24] and it involves a conformational analysis by molecular mechanics and the simulation of the EPR spectrum, based on the structural parameters shown in Fig. 4. The conformational analyses were performed in the same way as that described above for $[Cu_2L^3]^{2+}$ [an equatorial ammonia and two additional axial water molecules complete the co-ordination around the copper(II) centres; in Figs. 5 and 6 the axial water molecules are omitted for clarity]. The structural parameters of the two complexes are given in Table 5 and the two structures are plotted in Figs. 5 and 6.

The structure refined for $[Cu_2L^2]^{4+}$ is more than 9 kJ mol^{-1} more stable than all other conformers, while that determined

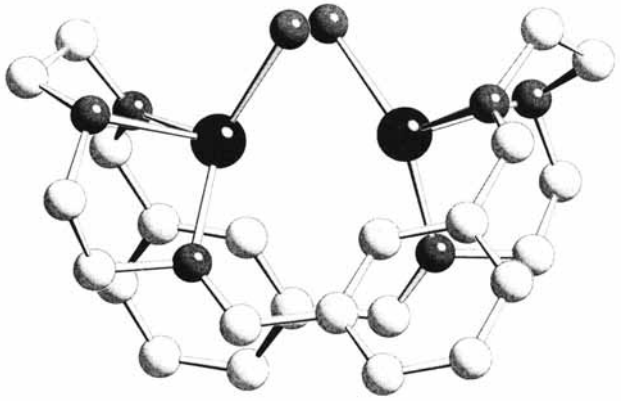

Fig. 2 SCHAKAL[21] plot of the lowest strain energy structure of $[Cu_2(Y)_2L^3]^{2+}$

Table 4 Strain-energy minimized (and observed) Cu(I)–N bond lengths (Å) and Cu–Cu separations (Å) for mixed amine–imine copper(I) complexes

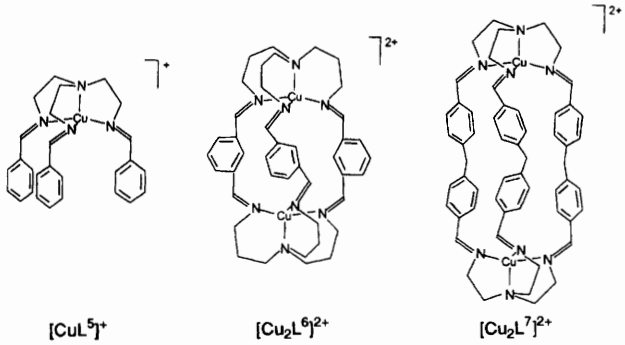

Structure	Strain energy/ kJ mol^{-1}	Cu(1)–N_{amine}/Å	Cu(1)–N_{imine}/Å	Cu–Cu/Å
$[Cu_2(NH_3)_2L^1]^{2+}$	56.37	2.192 (2.185)	2.034 (2.033)	6.3 (7.0)
$[CuL^5]^{+a}$	46.95	2.238 (2.232)	2.216 (2.210)	—
$[Cu_2L^6]^{2+b}$	107.79	2.279 (2.280)	2.022 (2.090)	4.1 (4.4)
$[Cu_2L^7]^{2+c}$	98.17	2.249 (2.245)	2.013 (1.980)	10.6 (11.0)

[a] Ref. 17. [b] Ref. 18. [c] Ref. 19.

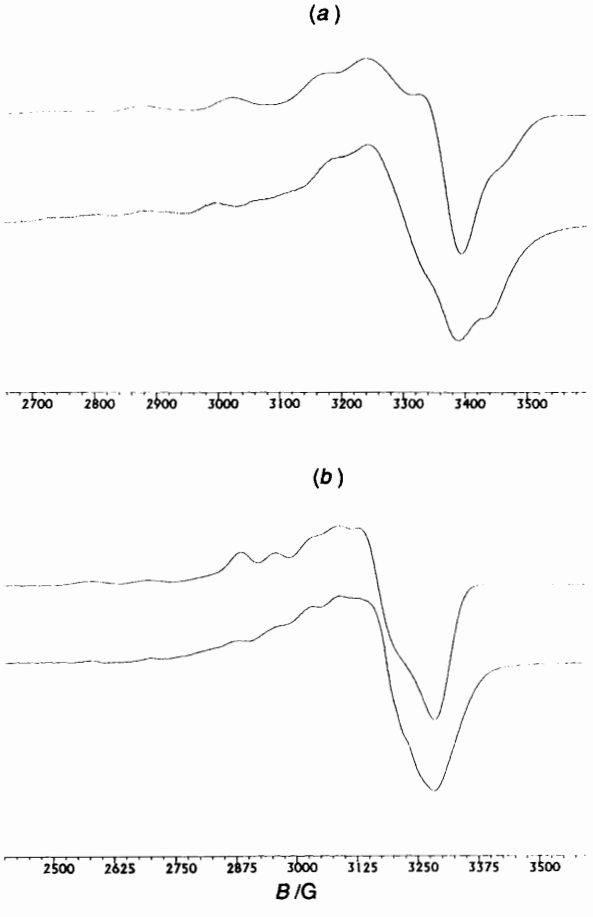

Fig. 3 Experimentally determined (bottom) and simulated (top) EPR spectrum of (*a*) $[Cu_2L^2]^{4+}$ at 9.548 GHz (r = 6.9 Å; $\xi = \eta = 90$, τ = 0°; $g_\perp$ = 2.06; $g_\parallel$ = 2.28; $A_\perp = 43 \times 10^{-4}$, $A_\parallel = 157 \times 10^{-4}$ cm^{-1}) and (*b*) $[Cu_2L^4]^{4+}$ at 9.303 GHz (r = 5.9 Å; ξ = 63, τ = 69, η = 5°; $g_\perp$ = 2.09, $g_\parallel$ = 2.40; $A_\perp = 34 \times 10^{-4}$, $A_\parallel = 131 \times 10^{-4}$ cm^{-1})

for $[Cu_2L^4]^{4+}$ is only 2 kJ mol^{-1} more stable than one conformer but more than 5 kJ mol^{-1} more stable than all the others. The second-lowest energy conformer of $[Cu_2L^4]^{4+}$ does not lead to a simulated EPR spectrum in agreement with that observed experimentally. Owing to the larger flexibility

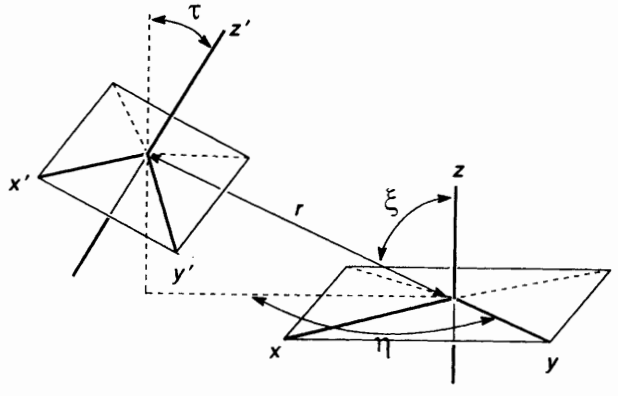

Fig. 4 Definition of the structural parameters used for the simulation of the EPR spectra

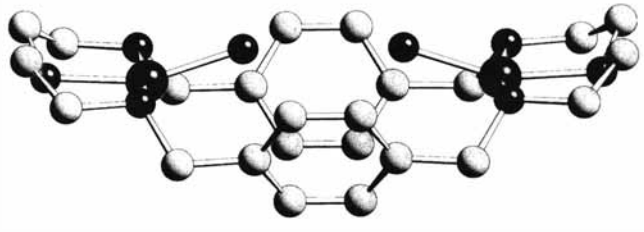

Fig. 5 SCHAKAL[21] plot of the calculated structure of $[Cu_2L^2]^{4+}$ (MM-EPR)

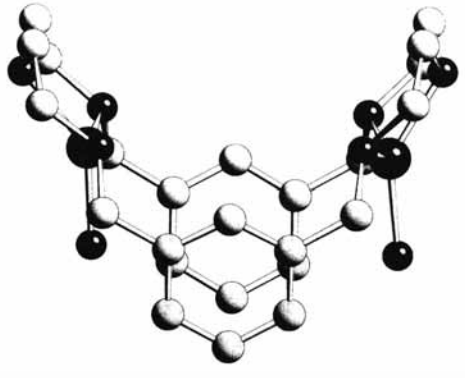

Fig. 6 SCHAKAL[21] plot of the calculated structure of $[Cu_2L^4]^{4+}$ (MM-EPR)

Table 5 Geometric parameters of the strain-energy minimized (MM) and solution structures (MM-EPR)

Structure	Cu–Cu/Å	ξ/°	τ/°	η/°	Strain energy/ kJ mol^{-1}
$[Cu_2L^2]^{4+}$ (MM)	6.9	90	0	90	52.41
$[Cu_2L^2]^{4+}$ (MM-EPR)	6.9	90	0	90	
$[Cu_2L^4]^{4+}$ (MM)	5.9	49	64	0	50.37
$[Cu_2L^4]^{4+}$ (MM-EPR)	5.9	63	69	5	

of the ligand backbones of the hexaamine macrocycles compared with the Schiff-base ligands, the difference between the Cu–Cu distances in $[Cu_2L^2]^{4+}$ (6.9 Å) and $[Cu_2L^4]^{4+}$ (5.9 Å) is noticeably smaller than that of the related dicopper(I) complexes. The calculated Cu–Cu separation of $[Cu_2L^2]^{4+}$ is confirmed by a preliminary crystal structure[25] (Cu–Cu separation of 6.95 Å) which contains two $[Cu_2L^2]^{4+}$ units linked by a pair of carbonate groups. Due to the interaction of the two $[Cu_2L^2]^{4+}$ units in the tetramer the relative orientation of the copper(II) chromophores is different in that molecule. Due to the instability of the μ-co-ordinated carbonate groups it is unlikely that this tetrameric structure is present in solution. The larger flexibility also results in pronounced differences in the geometries of the chromophores, with a tetrahedral twist of $\theta_{average} \approx 9°$ for $[Cu_2L^2]^{4+}$ (θ is the tetrahedral twist angle defined by two independent CuN_2 planes; $\theta = 0$ for planar and 90° for tetrahedral) and a significantly larger twist of $\theta_{average} \approx 40°$ for $[Cu_2L^4]^{4+}$. The spectroscopic parameters are in agreement with these structural properties. A reduction in $A_{\parallel}$ [157 *vs.* 131 ($\times 10^{-4}$) cm^{-1}] and a red shift of the electronic absorption maximum (16 230 *vs.* 15 480 cm^{-1}) are indicative of a larger deviation from planarity of the central chromophore in $[Cu_2L^4]^{4+}$.

Electrochemical properties

Cyclic voltammograms of $[Cu_2L^1]^{2+}$ in MeCN show a single quasi-reversible oxidation wave due to Cu^{II} centred at +0.54 V *vs.* Ag–AgCl. In contrast, the cyclic voltammogram of $[Cu_2L^3]^{2+}$ shows evidence of two quite well separated oxidation waves centred at +0.7 (irreversible) and +1.35 V (quasi-reversible), the first of these possibly involving the formation of an intermediate mixed-valence Cu^I–Cu^{II} species, supporting the existence of a much stronger Cu–Cu interaction in this complex, in agreement with the structural analysis. Corresponding cyclic voltammograms obtained from the analogous $[Cu_2L^6]^{2+}$, with the ligand derived from tris(2-aminoethyl)amine, also show two oxidation waves, but in this case separated by only 220 mV.[26] In the crystal structure of $[Cu_2L^6]^{2+}$, used in the force-field parameterization, the two copper atoms are separated by 4.4 Å. In $[Cu_2L^3]^{2+}$ the two corresponding oxidation waves are separated by 650 mV, a feature reflective of a stronger Cu–Cu interaction and a Cu–Cu distance somewhat smaller than that in $[Cu_2L^6]^{2+}$, thus supportive of the value (≈3.4 Å) obtained from the energy-minimized solution structure.

Cyclic voltammograms for $[Cu_2L^2]^{4+}$ and $[Cu_2L^4]^{4+}$ in dry MeCN each show a single quasi-reversible oxidation process centred at +0.99 V and a broad quasi-reversible reduction wave due to Cu^I centred at ≈ −0.4 V. These results are consistent with the stabilization of Cu^{II} in these saturated hexaamine derivatives and with the much smaller differences apparent in the solution structures of $[Cu_2L^2]^{4+}$ and $[Cu_2L^4]^{4+}$.

Conclusion

The redox properties and oxygen reactivity of the two isomeric dicopper(I) complexes $[Cu_2L^3]^{2+}$ and $[Cu_2L^1]^{2+}$ differ strongly. While the former shows tyrosinase-like oxygenation reactivity at one of the aromatic rings of the ligand *via* a rapid reaction with dioxygen, the latter forms an oxygen-stable complex that can easily be isolated and structurally characterized. The strain-energy-minimized solution structure of $[Cu_2L^1]^{2+}$ is in good agreement with the experimental crystal structure, with a Cu–Cu separation of 6.3 Å. The Cu–Cu distance found for $[Cu_2L^3]^{2+}$ is significantly shorter (≈3.4 Å) and indeed similar to that in tyrosinase (3.6 Å), a feature possibly largely responsible for the oxygen reactivity observed. From the determination of the solution structures of the dicopper(II) species of the related hexaamines, using a combination of EPR spectroscopy and molecular mechanics, the conformational analysis, based on molecular mechanics alone, could be confirmed, and this supports the structural analysis performed on the related dicopper(I) compounds, which are based on molecular mechanics alone. Despite the deficiencies that might be apparent in a conformational analysis based solely on molecular mechanics, the results show that the significantly shorter Cu–Cu separation found for $[Cu_2L^3]^{2+}$ is supported by the electrochemical data (evidence of a strong Cu–Cu interaction) and, moreover, a self consistency within the same type of deterministic conformational analysis, refined with a constant force field, for the four binuclear structures presented.

Experimental

CAUTION: Perchlorate salts are potentially explosive and should be handled with care.

Materials

All chemicals used for the preparative work were of reagent grade quality. Solvents used for spectroscopic and electrochemical measurements were of the required grade.

Synthesis

The ligands. The macrocycles L^1 and L^3 were prepared by the (2 + 2) condensation of terephthalaldehyde and isophthalaldehyde, respectively with 3-azapentane-1,5-diamine according to published procedures.[27] The ^1H and ^{13}C NMR spectra of L^3 in $CDCl_3$ are complex, suggesting the presence of tautomeric isomers of the Schiff base[28] deriving from reversible nucleophilic attack by secondary R_2NH at an imine carbon. However the ^1H and ^{13}C NMR spectra of L^1 in $CDCl_3$ are consistent with 100% of the tetraimine form. Characterization of L^1 and L^3 was on the basis of their ν_{CN} bands at 1645 and 1650 cm^{-1} respectively, and elemental analyses. The macrocyclic hexaamines L^2 and L^4 were obtained by reduction of L^1 and L^3 with sodium tetrahydridoborate in ethanol, using previously described procedures.[29] Both were isolated as their HBr salts and, following recrystallization from ethanolic HBr, characterized by ^1H, ^{13}C NMR and IR spectroscopy [absence of the ν_{CN} band] and by elemental analyses.

$[Cu_2(NCMe)_2L^1][ClO_4]_2$. The compound $[Cu(NCMe)_4]ClO_4$[30] (0.88 g, 2.75 mmol) in MeCN (30 cm^3) was added under argon to a stirred solution of L^1 (0.5 g, 1.244 mmol) in MeCN (50 cm^3). The mixture was refluxed for 2 h and the

golden orange precipitate filtered off, washed with MeCN and dried in a vacuum desiccator over silica gel. Over a period of several days at room temperature the filtrate slowly deposited red-orange crystals of $[Cu_2(NCMe)_2L^1][ClO_4]_2$ which were found to be suitable for crystal structure studies (see below). Subsequent analysis revealed that the red-orange crystals and the golden orange precipitate were of the same composition. Yield: 0.61 g, 0.75 mmol, 61% [Found: C, 41.40; H, 4.45; Cl, 8.55; N, 13.55. Calc. for $C_{28}H_{36}Cl_2Cu_2N_8O_8$ (M = 810.64): C, 41.50; H, 4.50; Cl, 8.75; N, 13.80%]; IR ($\tilde{\nu}$/cm^{-1}) 2210w (C≡N) and 1619s (C=N). ^{1}H NMR [300 MHz, $(CD_3)_2SO$, internal $SiMe_4$]: δ 2.07 (s, 6 H, MeCN), 2.85 (br, 4 H, CH_2), 3.14 (br, 4 H, CH_2), 3.75 (br, 4 H, CH_2), 3.87 (br, 4 H, CH_2), 4.50 (br, 2 H, NH), 8.25 (s, 8 H, C_6H_4) and 8.76 (s, 4 H, CH=N); ^{13}C NMR (75.47 MHz, ^{1}H-decoupled): δ 1.3 (MeCN), 45.7 (CH_2), 60.5 (CH_2), 118 (MeCN), 128.8 (unsubstituted ring C), 136.5 (substituted ring C) and 163.9 (C=N).

$[Cu_2(L^2)][ClO_4]_4\cdot H_2O$. An excess of $CuCO_3$ (0.2 g, 1.68 mmol) was added to a solution of $L^2\cdot 6HBr$ (0.5 g, 0.56 mmol) in distilled water (50 cm^3), and the suspension was stirred at room temperature for 3 h. The excess $CuCO_3$ was filtered off, and to the deep blue filtrate was added $NaClO_4$ (0.3 g, 2.8 mmol, in 5 cm^3 H_2O) at 0 °C. The blue solid that precipitated was filtered off and allowed to dry in a desiccator over silica gel. Yield: 62 mg, 0.065 mmol, 12% [Found: C, 30.35; H, 4.20; N, 8.75. Calc. for $C_{24}H_{40}Cl_4Cu_2N_6O_{17}$ (M = 953.21): C, 30.20; H, 4.20; N, 8.80%]. Molar conductance (1 × 10^{-3} mol dm^{-3} aqueous solution), Λ = 460 S cm^2 mol^{-1} (4:1 electrolyte). Electronic spectrum (H_2O): λ_{max} = 615 nm (ε = 125 dm^3 mol^{-1} cm^{-1} per Cu). μ_{eff} (18 °C) = 1.6 μ_B (≈1.48 × 10^{-23} J T^{-1}) per Cu.

$[Cu_2(L^4)][ClO_4]_4\cdot H_2O$. In a similar procedure to that described above for $[Cu_2(L^2)][ClO_4]_4\cdot H_2O$, a blue precipitate was isolated. Yield: 0.3 g, 0.31 mmol, 60% [Found: C, 30.65; H, 4.15; N, 8.85. Calc. for $C_{24}H_{40}Cl_4Cu_2N_6O_{17}$ (M = 953.21): C, 30.20; H, 4.20; N, 8.80%]. Molar conductance (1 × 10^{-3} mol dm^{-3} solution in H_2O) Λ = 440 S cm^2 mol^{-1} (4:1 electrolyte). Electronic spectrum (H_2O): λ_{max} = 646 nm (ε = 154 dm^3 mol^{-1} cm^{-1} per Cu). μ_{eff} (18 °C) = 1.53 μ_B (≈1.42 × 10^{-23} J T^{-1}) per Cu.

Crystallography

Crystal data for $[Cu_2(NCMe)_2L^1][ClO_4]_2$. $C_{28}H_{36}Cl_2Cu_2N_8O_8$, M = 810.64, triclinic, space group $P\bar{1}$, a = 10.5773(9), b = 10.8385(8), c = 7.9715(4) Å, α = 99.572(6)°, β = 91.698(7)°, γ = 108.952(6)°, U = 848.9(1) Å^3, Z = 1, D_c = 1.585 g cm^{-3}, λ(Cu-Kα) = 1.5418 Å, F(000) = 416, red plates 0.22 × 0.22 × 0.045 mm, μ = 35.08 cm^{-1}, $R(F_o)$ = 0.045, R' = 0.046 [$R = \Sigma(|F_o| - |F_c|)/\Sigma|F_o|$, $R' = (\Sigma w|F_o| - |F_c|)^2/(\Sigma wF_o^2)^{\frac{1}{2}}$], $w = 1/\sigma(F)^2$.

A suitable crystal of $[Cu_2(NCMe)_2L^1][ClO_4]_2$ was mounted on a glass fibre with cyanoacrylate resin. Lattice parameters at 21 °C were determined by least-squares fits to the setting parameters of 25 independent reflections, measured and refined on an AFC-7 four-circle diffractometer employing graphite-monochromated Cu-Kα radiation. Intensity data were collected in the range 1 < θ < 60°. Data reduction and application of Lorentz, polarization, absorption and decomposition corrections were carried out using the TEXSAN system.[31] The structure was solved by direct methods using SHELXS 86.[32] Hydrogen atoms were included at calculated sites with fixed isotropic thermal parameters. All other atoms with the exception of a disordered water molecule were refined anisotropically. Full-matrix least-squares methods were used to refine an overall scale factor, positional and thermal parameters. Neutral atom scattering factors were taken from international tables.[33] Anomalous dispersion effects were included in F_c;[34] the values for $\Delta f'$ and $\Delta f''$[35] and the values for the mass attenuation coefficients are taken from the literature.[36] All calculations were performed using TEXSAN[31] and plots were drawn using ORTEP.[21]

Complete atomic coordinates, thermal parameters and bond lengths and angles have been deposited at the Cambridge Crystallographic Data Centre. See Instructions for Authors, *J. Chem. Soc., Dalton Trans.*, 1996, Issue 1.

Physical methods

Infrared spectra (KBr pellets) were measured with a Perkin-Elmer 1710 FT instrument, UV/VIS on solutions in 1 cm quartz cuvettes using Perkin-Elmer Lambda 5 or Philips PU8256 scanning spectrophotometers. Conductance measurements were made with an AGB 1000 conductivity meter using 1 × 10^{-3} mol dm^{-3} solutions of the metal complexes in distilled water. Magnetic measurements were recorded on a Johnson Matthey mini balance using $Hg[Co(NCS)_4]$ as the calibrant (χ_g = 16.77 × 10^{-6} cgs at 18 °C). Cyclic voltammograms were recorded using a PAR model 170 electrochemistry system on either aqueous (0.1 mol dm^{-3} $NaClO_4$) or MeCN solutions (0.1 mol dm^{-3} NBu_4PF_6) of the metal complexes. A standard three-electrode cell was used comprising glassy carbon or platinum disc working, platinum wire counter and saturated calomel (or Ag–AgCl) reference electrodes. Proton and ^{13}C NMR spectra were recorded on a Bruker AM-300 instrument at 300 MHz and 75.47 MHz respectively and EPR spectra [10^{-3} mol dm^{-3} dimethylformamide–water (1:2), frozen solutions at 150 K] with a Bruker ESP 300E instrument (Bruker ER 041 XK X-band microwave bridge). The spin-Hamiltonian parameters, the copper(II)–copper(II) separation and the relative orientation of the chromophores of the dipole–dipole coupled binuclear copper(II) complexes were determined by simulation of the ΔM_s = 1 resonances with the computer program DISSIM.[37] Molecular mechanics calculations were performed with MOMEC[38] using a published force field.[17] New parameters for Cu^I–ligand atom interactions are given in Table 4. Two modifications that were necessary to model the copper(I) complexes accurately are: (*i*) the force constant k for the torsion angle around the benzene carbon–carbon bonds was set from 0.003 to 0.015 mdyn Å (dyn = 10^{-5} N) and (*ii*) the strain-free bond length of the nitrogen–carbon bond of amines co-ordinated to copper(I) has to be different from that of copper(II) complexes [1.490 Å and 1.460 Å for copper(II) and copper(I), respectively].

Acknowledgements

We gratefully acknowledge financial support by the Deutsche Forschungsgemeinschaft (DFG), the Deutsche Akademische Austauschdienst (DAAD) and the British Council (British–German Academic Research Collaboration Project 484).

References

1 *Bioinorganic Chemistry of Copper*, eds. K. D. Karlin and Z. Tyeklár, Chapman and Hall, New York, London, 1993.
2 *Bioinorganic Catalysis*, ed. J. Reedijk, Marcel Dekker, New York, Basel, Hong Kong, 1993.
3 *Crown Compounds – Toward Future Applications*, ed. S. R. Cooper, VCH, Weinheim, 1993.
4 P. A. Vigato, S. Tamburini and D. E. Fenton, *Coord. Chem. Rev.*, 1990, **106**, 25.
5 E. I. Solomon, M. J. Baldwin and M. D. Lowery, *Chem. Rev.*, 1992, **92**, 521.
6 T. N. Sorrell, *Tetrahedron*, 1989, **45**, 3.
7 K. D. Karlin, P. Ghosh, R. W. Cruse, A. Farooq, Y. Gultneh, R. R. Jacobson, N. J. Blackburn, R. W. Strange and J. Zubieta, *J. Am. Chem. Soc.*, 1988, **110**, 6769.
8 K. D. Karlin, Z. Tykelar, A. Farooq, M. S. Haka, P. Ghosh, R. W. Cruse, Y. Gultneh, J. C. Hayes, P. J. Toscano and J. Zubieta, *Inorg. Chem.*, 1992, **31**, 1436.

9 S. M. Nelson, E. Esho, A. Lavery and M. G. B. Drew, *J. Am. Chem. Soc.*, 1983, **105**, 5693.
10 P. Sharma and G. S. Vigei, *Inorg. Chim. Acta*, 1984, **88**, 29.
11 K. D. Karlin, M. S. Nazir, B. I. Cohen, B. W. Cruse, S. Kaderli and A. D. Zuberbuhler, *J. Am. Chem. Soc.*, 1994, **116**, 1324; K. D. Karlin, J. C. Hayes, Y. Gultneh, B. W. Cruse, J. W. McKown, J. P. Hutchinson and J. C. Zubieta, *J. Am. Chem. Soc.*, 1984, **106**, 2121.
12 L. Casella and L. Rigoni, *J. Chem. Soc., Chem. Commun.*, 1985, 1668.
13 O. J. Gelling, F. van Bolhuis, A. Meetsma and B. L. Feringa, *J. Chem. Soc., Chem. Commun.*, 1988, 552.
14 R. Menif, A. E. Martell, P. J. Squattrito and A. Clearfield, *Inorg. Chem.*, 1993, **29**, 4723.
15 P. V. Bernhardt, P. Comba, T. W. Hambley, S. S. Massoud and S. Stebler, *Inorg. Chem.*, 1992, **31**, 2644.
16 C. K. Johnson, ORTEP, A Thermal Ellipsoid Plotting Program, Oak Ridge National Laboratories, Oak Ridge, TN, 1965.
17 P. V. Bernhardt and P. Comba, *Inorg. Chem.*, 1992, **31**, 2638.
18 E. C. Alyea, G. Ferguson, M. C. Jennings and Z. Xu, *Polyhedron*, 1990, **9**, 739.
19 M. P. Ngwenya, A. E. Martell and J. Reibenspies, *J. Chem. Soc., Chem. Commun.*, 1990, 1207.
20 J. Jaazwinski, J.-M. Lehn, D. Lilienbaum, R. Ziessel, J. Guilhem and C. Pascard, *J. Chem. Soc., Chem. Commun.*, 1987, 1691.
21 E. Keller, SCHAKAL 92, *J. Appl. Crystallogr.*, 1989, **22**, 19.
22 K. A. Magnus, H. Tonthat and J. E. Carpenter, *Chem. Rev.*, 1994, **94**, 727; B. Hazes, K. A. Magnus, C. Bonaventura, J. Bonaventura, Z. Dauter, K. H. Kalk and W. G. J. Hol, *Protein Sci.*, 1993, **2**, 597; A. Volbeda and W. G. J. Hol, *J. Mol. Biol.*, 1989, **206**, 249, 531.
23 K. A. Magnus, B. Hazes, H. Tonthat, C. Bonaventura, L. Bonaventura, Z. Dauter, K. H. Kalk and W. G. J. Hol, *Proteins: Struct. Funct. Genet.*, 1994, **19**, 302; H. Tonthat and K. A. Magnus, *J. Inorg. Biochem.*, 1993, **51**, 65.
24 P. Comba and P. Hilfenhaus, *J. Chem. Soc., Dalton Trans.*, 1995, 3269.
25 P. Comba, P. Hilfenhaus, T. W. Hambley and D. T. Richens, unpublished work.
26 L. Qin, M. McCann and J. Nelson, *J. Inorg. Biochem.*, 1993, **51**, 633.
27 R. Menif and A. E. Martell, *J. Chem. Soc., Chem. Commun.*, 1989, 1521.
28 R. W. Hay, D. T. Richens, G. Wyllie, A. Danby and T. Clifford, *Transition Met. Chem.*, 1995, **20**, 220; M. Pietraszkiewicz and R. Gasiorowski, *Chem. Ber.*, 1990, **123**, 405.
29 D. Chen and A. E. Martell, *Tetrahedron*, 1991, **34**, 6895.
30 J. v. Rijn and J. Reedijk, *J. Chem. Soc., Dalton Trans.*, 1987, 2579.
31 TEXSAN, Crystal Structure Analysis Package, Molecular Structure Corporation, Houston, TX, 1985, 1992.
32 G. M. Sheldrick, SHELXS 86, *Crystallographic Computing 3*, eds. G. M. Sheldrick, C. Krüger and R. Goddard, Oxford University Press, 1986, pp. 175–189.
33 D. T. Cromer and J. T. Waber, *International Tables for X-Ray Crystallography*, Kynoch Press, Birmingham, 1974, vol. 4.
34 J. A. Ibers and W. C. Hamilton, *Acta Crystallogr.*, 1964, **17**, 781.
35 D. C. Creagh and W. J. McAuley, *International Tables for Crystallography*, ed. A. J. C. Wilson, Kluwer Academic Publishers, Boston, 1992, vol. C, table 4.2.6.8, pp. 219–222.
36 D. C. Creagh and J. H. Hubbell, *International Tables for Crystallography*, ed. A. J. C. Wilson, Kluwer Academic Publishers, Boston, 1992, vol. C, table 4.2.4.3, pp. 200–206.
37 T. D. Smith and J. R. Pilbrow, *Coord. Chem. Rev.*, 1974, **13**, 173.
38 P. Comba, T. W. Hambley and N. Okon, MOMEC, A molecular mechanics program for coordination compounds, adapted to HyperChem™, Altenhoff and Schmitz, Dortmund, 1995.

Received 27*th July* 1995; *Paper* 5/04989J